9
Gas–Liquid-phase Reactions: Addition

Claude de Bellefon

Gas–solid additions such as hydrogenations and selective oxidations are covered in other chapters of this book and so will not be commented upon in this chapter.

Many reviews and books containing information on multiphase addition reactions have been published [1–3]. Often, they refer to publications in conference proceedings which are not available on-line. In this chapter, it is intended when possible to refer to original work published in readily accessible scientific journals and including some patents.

Whereas many types of additions are found in monophasic, i.e. liquid-phase, systems, most multiphase addition reactions in structured reactors are in fact H_2 additions, i.e. hydrogenations with some examples of oxygen addition across dienes ([4 + 2] cycloadditions). Hydrogen itself is a loosely reactive molecule and requires activation through a catalyst, either molecular or solid, thus driving to gas–liquid and gas–liquid–solid multiphase systems. Other challenging issues for hydrogenations are the low solubility of hydrogen, which calls for efficient mass transfer, and the exothermicity of hydrogenations, ranging from $100\,kJ\,mol^{-1}$ for hydrogenation of C=O bonds to $550\,kJ\,mol^{-1}$ for nitro derivatives, which call for efficient heat removal [4]. These issues are fundamental motivations to using structured reactors, albeit other motivations such as catalyst screening, kinetic and deactivation studies, safety regulations or just experimentation with new microstructures are most often encountered as the actual motivations.

The chapter is organized in two parts. The first section is devoted to a short description of typical microstructured reactors used for multiphase additions. The other sections are then organized according to reaction types, i.e. addition across carbon–carbon and carbon–oxygen double bonds, and other additions.

9.1
Types of Reactors

Many types of structured reactors may be used to perform multiphase additions. Requirements are to ensure efficient contact between the phases (gas, liquid and
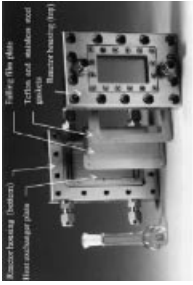
solid), to achieve a flexible residence time, from seconds to hours, to provide a large range of operating conditions (temperature, pressure) and good chemical compatibility (corrosion issue) [1].

Two main principles are used to ensure efficient fluid–fluid contacting: (i) dispersion of gas bubbles or liquid droplets in a liquid continuous phase: this principle has been used in capillaries and in monolith reactors where it leads to a segmented gas–liquid or liquid–liquid flow called Taylor flow, and for the generation of emulsions containing microbubbles or droplets; and (ii) fluid film contacting, where a liquid film is contacted with a gas layer either with gravity-driven liquid flow (falling film) or with pressure-driven horizontal gas–liquid film contactors. These two contacting principles have been turned into actual laboratory and small-scale production equipment via a smart arrangement of parallel reaction channels fed by microstructured gas and liquid distributors generating either microbubbles or fluid sheets and incorporation of solid catalysts when required. The main characteristics of these reactors, as given in the literature reports, are depicted in Table 9.1. For each reactor type, the construction material and typical dimensions of the reaction volume are given together with reactor's performances such as pressure, temperature, flow rate of liquid and liquid residence time. The coefficient $k_l a$ which characterizes the gas–liquid mass transfer is also provided when available. For heterogeneous catalyzed reactions, the way in which the solid catalyst is arranged in the reactor, i.e. deposition on the walls (wall-coated) [5], or as a finely divided powder, is indicated. Many channel-type reactors can be operated in both ways, with a washcoated or a powder catalyst. It is believed that all these indications may be useful for the proper choice of a (micro)structured reactor for multiphase addition reactions. Note that the photographs and schemes are shown as illustrations and are not intended to restrict the technology developed by other research groups.

The falling film principle was used for the design of reactor **R1**. This reactor can be operated over fairly large ranges of temperature and pressure. A maximum liquid throughput of 25 cm^3 min^{-1} can be achieved with a new version of this device [6]. The main drawback is the very short residence time. Such a residence time associated with the large mass transfer coefficient and the heat exchange capabilities make this reactor particularly well designed for fast and exothermic reactions such as some hydrogenations and fluorinations [7]. For solid catalyzed reactions, a layer of the catalyst, typically 10–30 μm thick, is deposited on the microstructured plate [5]. The total amount of catalyst available is small, however, in the range of a few milligrams, and with a low solid hold-up ($m^3_{cat.} m^{-3}_{channels}$). The gas–liquid mass transfer coefficient $k_l a$ has been measured and/or estimated to be in the range 3–8 s^{-1} using several methods [8].

Reactor **R2** is also based on the film contacting principle. It depicts two cavities of ca. 100 μL separated by a nickel mesh with openings of 3–5 μm. The total gas–liquid interface is thus ca. 2000 m^2 m$^{-3}_{liquid}$. In contrast to **R1**, the liquid film is not gravity but pressure driven with e.g. a syringe pump. This reactor presents many advantages such as high liquid residence time, batch mode, liquid–liquid and gas–liquid–solid operations. The main drawback is the difficulty in maintaining a stable gas–liquid interface during operations, even in the presence of a mesh which helps. Thus, **R3**
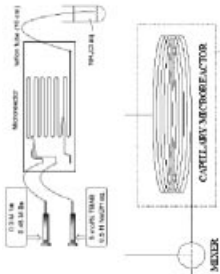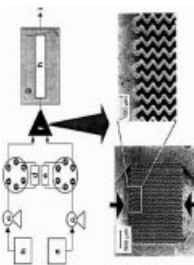
Table 9.1 Microstructured reactors mostly used for multiphase addition reactions.

Film contactors

	Example	Characteristics		Application^a	Reference
R1		Material	Stainless steel	GL	[26]
		No.	64 channels	GLS	[27]
		$W \times D \times L$	$300 \times 100\,\mu m \times 78\,mm$	GLS	[8, 28] photo
		T, P	-42–$130\,°C$, 1–6 bar		
		Q_L	0.12–2 cm^3 min^{-1}		
		τ_r	14–17 s		
		Cat.	Wall-coated		
				O$_2$ addition	
				H$_2$ addition to C=C	
				Hydrogenation nitro	
R2		Material	Glass and SS	GL	[29]
		No.	1 cavity	LL	[30] photo
		$W \times D \times L$	$- \times 155\,\mu m \times 33\,mm$	GL	[31]
		T, P	20–60 °C, 3–40 bar	GLS	[32]
		Q_L	25–200 μL min^{-1}	GLS	
		τ_r	0.6–5 min or batch		
		Cat.	Wall-coated		
				Characterization	
				Asymmetric hydrogenation	
				Asymmetric H$_2$ addition to C=O	
				H$_2$ addition to C=C	

(*Continued*)

Table 9.1 (*Continued*)

	Example	Characteristics		Application[a]		Reference
Segmented flow	R3		Material	Si, glass or PTFE	GL	O_2 addition	[11]
			No.	1–8	GLS	H_2 addition to C=C	[12] photo
			d_h	170–1000 µm	GLS	$H_2 + O_2 \rightarrow H_2O_2$	[33]
			T, P	20–60 °C, 1–20 bar	GLL	H_2 addition to C=O	[13] photo
			Q_L	1–1000 µL min^{-1}			
			τ_r	2–3 min			
			Cat.	Wall-coated			
	R4		Material	Al_2O_3	GLS	H_2 addition to C=C	[34–38]
			No.	400–100 cpsi	GLS	Hydrogenation nitro	[39]
			I.d. ×L	0.2–2 mm × 0.3–3 m	GLS	Hydrogenation AQ	[40]
			T, P	25–70 °C, 1–25 bar			
			Q_L	0.4–10 cm^3 min^{-1}			
			τ_r	0.1–280 s			
			Cat.	Wall-coated			
Foam contactor	R5		Material	Glass or SS	GL	Asymmetric H_2 addition to C=C	[41–43] photo
			No.	1 tube			
			I.d.	3 mm			
			L	Up to 3 m			
			T, P	20–70 °C 1–11 bar			
			Q_L	Up to 10 cm^3 min^{-1}			
			τ_r	<12 min			

Packed-bed channels

R6

Material	SS	H₂ addition to C=C	GLS	[44, 45]
No.	1 tube	Hydrogenation nitro	GLS	[46, 47]
I.d.×L	Variable	Kinetics		
T, P		Hydrogenation AQ	GLS	[48]
Q_L		$H_2 + O_2 \rightarrow H_2O_2$	GLS	[49]
τ_r		Kinetics		
Cat.	Packed powder			

R7
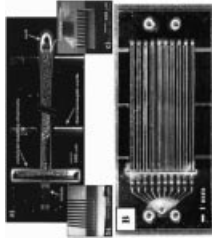
Material	Silicon	Hydrogenation C=C	GLS	[17] photo, [50]
No.	1–10 channels	$H_2 + O_2 \rightarrow H_2O_2$	GLS	[33]
W×D×L	$625 \times 300\,\mu m \times 20\,mm$	Hydrogenation nitro	GLS	[46]
T, P	20–235 °C, 1–100 bar			
Q_L	10–$100\,\mu L\,min^{-1}$			
τ_r	1–50 s			
Cat.	Packed powder			

R8
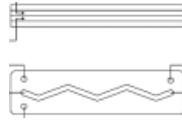
Material	SS	H₂/CO addition to C=C	GL	[51] photo
No.	1 channel	H₂ addition to aromatics	GLS	[52]
W×D×L	1 or 2 mm	H₂ addition to C=C	GLS	[45]
T, P	20–90 °C, 1–40 bar			
Q_L	$15\,cm^3\,min^{-1}$			
τ_r	–			
Cat.	Powder/molecular			

[a] In all tables, GL = gas–liquid, GLL = gas–liquid–liquid, GLS = gas–liquid–solid, LL = liquid–liquid.

cannot be operated unattended, which limits applications. Gas–liquid–solid reactions can be performed through the deposition of a thin layer of a solid catalyst on the bottom of the liquid cavity. The heat transfer capabilities have never been investigated but the overall design of **R2** is not well suited for heat exchange. This reactor is thus well suited for slow reactions for which a low inventory of material is required. Albeit the design of **R2** has been patented [9], it is not commercially available.

Both reactor types **R3** and **R4** use the segmented flow (Taylor) principle. They are divided into two categories: **R3** has very small channels (<1 mm) and **R4** are monolith reactors (honeycomb), well developed on the laboratory scale with at least one example of industrial application. Category **R3** includes single-channel and multiple-channel reactors [10], etched in silicon [10] or glass [10, 11], with wall-coated or immobilized catalysts in the case of gas–liquid–solid additions [12], and capillary microreactors for gas–liquid–liquid systems [13].

One major advantage of this class of reactor is the facility to set a segmented flow fluidic system with a simple glass capillary (e.g. a GC column) or a 1/16 PTFE or stainless-steel tube. However, scale-up or numbering-up is not as easy, multiple channel chips requiring precise machining/etching for generating the Taylor flow and for equal distribution of the flow in the channels. Reactor type **R4** can be viewed as a scaled-up version of **R3** albeit with larger channels, poor heat exchange capabilities and possible uneven flow distribution in the channels. It is not intended to cover fully the large amount of work published on monolith reactors but rather to give some basic information on how they can be used. A review covering monoliths as multiphase reactors has been published [14]. Information may also be found in books [15]. Hydrodynamics and mass transfer aspects have also been reviewed [16].

In foam contactors **R5**, a gas–liquid foam is generated using a micromixer and travels in a delay loop. Depending on the gas and liquid flow rates, gas bubbles as small as $100\,\mu m$ are generated, leading to a high gas–liquid interfacial area ($5000\,m^2\,m_{foam}^{-3}$) with a high gas hold-up (up to 80%). However, applications are limited by the nature of the liquid layer since an aqueous phase containing a surface-active agent is required to generate and to prevent the bubbles from coalescing before the desired conversion has been achieved.

Reactors **R6** and **R7** are based on the same principle: a gas–liquid mixture is forced to flow through a packed bed of a calibrated powder catalyst. They have many common features but have been classified in two categories: in **R6** the reactor body is just a simple tube, whereas in **R7** it is a machined (etched) silicon or glass device. As a consequence, **R6** reactors most often display a single channel whereas **R7** can be scaled-out to multichannel devices to reach higher throughputs. Both **R6** and **R7** are specifically designed for three-phase reactions, the typical catalyst particle mean diameter being in the range $30–150\,\mu m$. Several recent publications have reported on fairly high gas–liquid mass transfer coefficients $k_l a$ ($2–9\,s^{-1}$) for such microscale packed-bed reactors, confirming the pioneering work of Jensen's group in the development of reactor type **R7** [17]. It is stated that a segmented gas–liquid flow develops in such a packed bed [18], but hydrodynamic studies are lacking, in striking contrast to the situation with the well-studied gas–liquid Taylor flow. As a

consequence, no good reactor model is available and scale-up or scale-out cannot be modeled. However, for the practical use of **R6** and **R7** contactors, the difficult step of particle incorporation in the reactor body has been demonstrated [17, 19], and the only drawback seems to be the need for well-calibrated catalyst particles.

Of course, not all multiphase microstructured reactors are presented in Table 9.1. Either because they have attracted (too?) little interest, because they may have been qualified as microreactors in spite of their overall size but cannot be considered as "microstructured", or because they combine several contacting principles. Examples are a reactor developed by Jensen's group featuring a channel equipped with posts or pillars, thus resembling more a packed bed but with a wall-coated layer of catalyst [20], and a "string" catalytic reactor proposed by Kiwi-Minsker and Renken [21], that may applied to multiphase reactions.

9.2
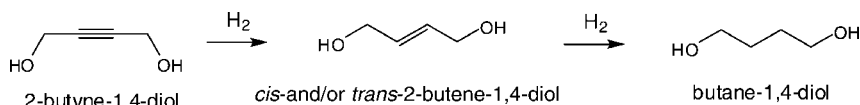## Additions of H₂, O₂, O₃ and CO/H₂ Across C=C

Many reports have described hydrogenations of C=C bonds (Table 9.2). In these reports, it is generally not intended to achieve attractive production numbers, but rather to use model reactions, either fast and/or exothermic, in order to characterize and demonstrate better the capabilities of microstructured multiphase reactors. Consequently, conversions are generally not high and the target substrates are not of great synthetic interest. However, these studies are worth mentioning since all the devices described may be adapted to reach higher conversions, e.g. operated at lower flow rates.

Cyclohexane hydrogenation was first used by Jensen's group as a demonstration reaction, to determine the global hydrogen transfer coefficient from the gas phase to the catalyst [17]. A platinum on alumina catalyst (1–5 wt.%) shaped as small particles (50–75 μm) was used with pressure (1–2.5 bar) and temperatures close to room conditions. A conversion below 16% was maintained in order to determine the mass transfer coefficient. With a typical quantity of 40 mg in the 15 × 40 × 0.5 mm silicon etched 10-channel reactor, cyclohexane production ranging from 0.2 to 0.3 g per day was obtained. The same experiment was also used recently but at higher pressure (51 bar) and temperature (75 °C) and using a palladium catalyst (2 wt.% on silica/alumina) [50]. With a single-channel reactor containing as little as 1.5 mg of catalyst, productions up to 0.35 g per day at 35% conversion were obtained. The higher production is probably due to both the higher activity of the palladium catalyst and the harsher operating conditions. In both experiments, serious mass transfer limitations were evidenced, as demonstrated by the very low measured activation energy (ca. 11 kJ mol^{-1}). Cyclohexane hydrogenation was also performed in a micro-falling film reactor (64-channel plate) charged with a Pd/alumina catalyst [27]. Conversions up to 65% were obtained at 65 °C and ambient pressure, albeit with a diluted feed of cyclohexane in toluene, with a cyclohexane production of ca. 0.5 g h^{-1}. In these studies, the exothermic character of cyclohexene hydrogenation ($\Delta H = -118$ kJ mol^{-1}) was mentioned but no temperature measurements were performed.

Table 9.2 Additions across carbon–carbon double bonds.

| Reaction	Type	Conditions	Motivation/requirements	Substrate	Reactor	Reference
H$_2$ additions (hydrogenations)	GLS	20–100 °C 1–100 bar	Demonstration High-pressure	Cyclohexene	R7	[17, 50]
		Washcoat or powder 1 s–5 min	Deactivation	Cyclohexene	R1	[27]
			Demonstration Characterization	α-Methylstyrene	R2	[30, 32]
			Thermal	Styrene 1-Octene	R4	[34, 37, 38]
			Selectivity	α,β-Unsaturated ketones Conjugated dienes Terminal and internal C=C	R3	[12]
	GL	20–70 °C 1–11 bar Molecular 1–30 min	Screening of chiral catalysts Kinetics Comparison with batch	(Z)-Methyl acetamidocinnamate	See text R2 R5	[53] [30] [41–43]
H-transfer addition	LL	70 °C Molecular 2–20 s	LL mass transfer	Dimethyl itaconate reduction	–	[54]
H$_2$/CO addition, hydroformylation	GLL	Molecular	Enhanced GL mass transfer	Hydroformylation of 1-octene	–	[55]
	GL	60–90 °C 15–30 bar Molecular	Demonstration Intensification Selectivity	Hydroformylation of cyclododecatriene	R8	[51]
Oxygen additions	GL	10–15 °C O$_2$, $h\nu$, Rose Bengal O$_3$, no catalyst 0.3 s	Safety demonstration Selectivity Safety Kinetics	[4 + 2] cycloaddition to Cyclopentadiene [4 + 2] cycloaddition to α-terpinene 1-Decene	R1 R3 See text	[26] [11] [20]

Scheme 9.1 Reaction scheme for the hydrogenation of 2-butyne-1,4-diol [38].

The hydrogenation of α-methylstyrene is very fast and was used to characterize mass transfer from the gas phase to the solid catalyst in a mesh contactor [30, 32]. With a Pd/alumina (1 wt.%) catalyst content as low as 25 mg, production of cumene of up to 0.76 g per day was achieved with 32% conversion of α-methylstyrene at 5 bar and 35 °C.

Monolith reactors were probably the first structured reactor type to be used for gas–liquid-solid three-phase reactions [14, 15]. With channel widths in the region of 1000 μm (400 cpsi), Taylor flow can be obtained, thus favoring external mass transfer. The hydrogenation of a mixture of styrene and 1-octene in toluene (0.5 : 0.5 : 99 wt.%), as a model charge for hydrotreatment reactions, was performed in a single tube washcoated with an Ni/alumina catalyst at ca. 60 °C and 15 bar pressure [34, 37]. As expected, almost complete conversion of the alkenes was achieved at high residence time, the conversion of the very reactive styrene always being higher than that of 1-octene. From the published data, an ethylbenzene production of ca. 3 g per day in the single-channel monolithic reactor of 1.2 cm³ may be estimated. Scale-up by using all channels of the monolith require the solving of potential maldistribution issues and is still to be demonstrated.

This last issue was tackled in a recent paper [38]. The hydrogenation of 2-butyne-1,4-diol was conducted at 55 °C and 2 bar pressure in monolithic reactor containing more than 5000 channels (1 mm) with a total diameter as large as 10 cm, equipped with a co-current downflow gas–liquid distributor. The results reveals that in the monolith reactor the selectivity for the intermediate 2-butene-1,4-diol (Scheme 9.1) can be kept very high (99.6%) even at quantitative substrate conversion, a much better value than in traditional stirred-tank or trickle-bed reactors (<95%). Since the Pd catalysts used in the different reactors are different, with much better dispersed Pd particles in the monolith reactor, the observed better selectivity is partly due to the intrinsic properties of the catalyst. The productivity numbers of the different reactors are not discussed.

A single-channel reactor (200 × 100 μm, 45 cm in length) with Pd-immobilized catalyst was obtained in several steps from functionalization of the channel walls and crosslinking polymerization of microencapsulated Pd [12]. The channel reactor was then operated in the annular flow mode where only gas is passing in the center of the channel, the liquid forming a very thin layer (18 μm) at the wall. Under very smooth conditions (room temperature and pressure) and short residence time, the C=C bond of various substrates (Scheme 9.2) was reduced with quantitative yields,
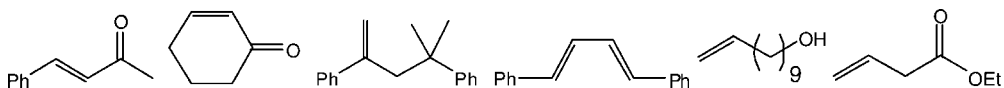

Scheme 9.2 Typical substrates for the single-channel reactor hydrogenation using Pd-immobilized catalyst [12].

excepted for 4-phenyl-2-butanol. Although a space–time yield 140 000 higher than those obtained in ordinary laboratory flasks is claimed, the actual productivities of the single-channel reactor are very small, in the range 0.02–0.06 g per day, depending on the substrates. This device was also used for deprotection (O−Bn and NH−Z bond cleavage) and for C≡C triple bond hydrogenation (see below).

The first gas–liquid asymmetric hydrogenation using a microstructured device was reported in 2000. It was based a combination of dynamic sequential operations with pulse injections and a reactor based on the "micromixer + tube" concept [43]. The kinetic investigation of the asymmetric hydrogenation of methyl (Z)-α-acetamidocinnamate with a rhodium/(S, S)-BDPPTS catalyst in an aqueous phase was also performed with this device. Up to 214 tests were performed in a short time and with an average inventory of Rh per test as low as 14 μg [42]. A microstructured single-channel helicoidal falling film reactor was used to study the asymmetric hydrogenation of prochiral substrates at temperature close to ambient (20–35 °C), 1 bar pressure and residence time in the range 3–22 min [53]. The screening of molecular rhodium/chiral diphosphine catalysts, with a library of 18 chiral phosphines (Scheme 9.3), for the asymmetric hydrogenation of methyl (Z)-α-acetamidocinnamate and other prochiral substrates has been performed.

This tool is obviously designed for investigation purposes and the very small reaction volume of 14 μL leads to an average inventory of Rh per test as low as 0.1 μg. The screening of rhodium/chiral diphosphine catalysts, with a library of 20 chiral phosphines, for the asymmetric hydrogenation of methyl (Z)-α-acetamidocinnamate was also investigated with a mesh-type gas–liquid contactor [30]. The effect of hydrogen pressure on the enantiomeric excess (ee) was investigated for (R, R)-diop,
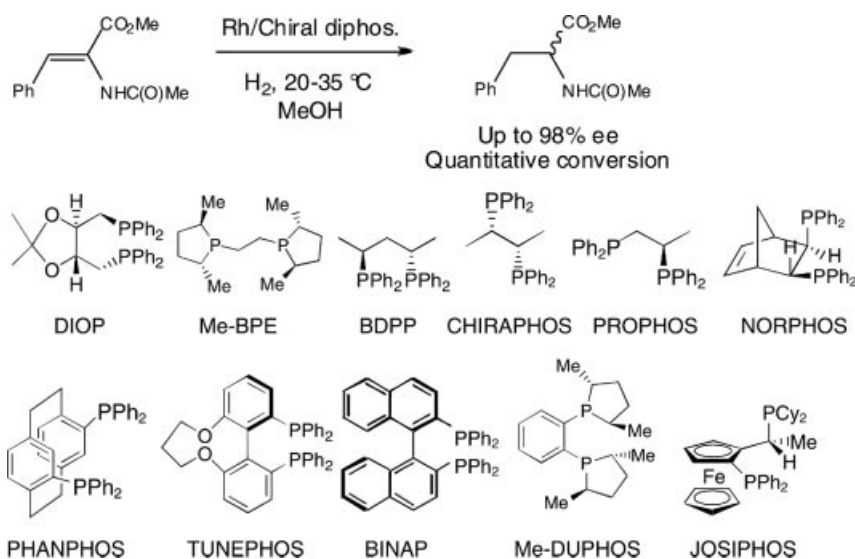
Scheme 9.3 Reaction scheme and selected members of the library of chiral phosphines investigated using the helicoidal falling film reactor [30, 53].
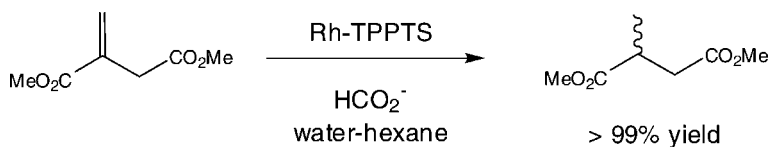
Scheme 9.4 H-transfer reduction of C=C bonds with biphasic liquid–liquid catalysis [54].

higher pressures (10 bar) being detrimental to the *ee*, whereas for other chiral diphosphines beneficial effects may be observed [22].

Hydrogen addition across the C=C bond of dimethyl itaconate was performed with sodium formate in aqueous solution as an H-transfer reagent (Scheme 9.4) [54]. In this reaction, the substrate is in the organic layer whereas the catalyst and the formate are in the aqueous phase where the reaction takes place. In such a liquid–liquid biphasic system, mass transfer may be an issue. A 43% conversion was obtained in the microstructured reactor while benchmarking with a traditional batch vessel afforded quantitative conversion (>99%). This was attributed to the poor mass transfer coefficient in the microdevice, which was originally designed to resolve heat transfer issues.

Only two examples of H_2/CO addition to alkenes (hydroformylation) in microstructured reactors have been reported. One of the largest industrial processes uses a three-phase (gas–liquid–liquid) reaction system, with a water-soluble catalyst. Such a process allows easy catalyst recovery by decantation. A limit for this process, however, is the use of loosely soluble higher alkenes in aqueous media. The use of microreactors was thought to offer a solution for process intensification, because of their superior intrinsic interface areas between different phases [55]. A capillary microreactor was used to conduct the hydroformylation of 1-octene. The published abstract, however, is insufficiently informative for further discussion. Hydroformylation can also be conducted in a gas–liquid system with an HRh(CO)(PPh$_3$)$_3$ molecular catalyst. A heat-exchange single-channel "milli-structured" reactor was used for the solvent-free hydroformylation of cyclododecatriene (CDDT) at 50–85 °C and 12–40 bar pressure [51]. The advantage of such an HEx reactor is the facility to scale-up to production units while keeping the advantages of heat exchange and mass transfer capabilities. The HEx reactor proved to offer slightly better selectivity in the desired monoaldehyde product (60% yield at 94% conversion of CDDT) with the same *Z:E* ratio (1 : 13) compared with a traditional tank reactor (Scheme 9.5). However, a ca. 10-fold improvement in productivity was obtained in the HEx reactor, which was attributed to the better mass transfer capability.

The [4 + 2] addition of singlet oxygen to conjugated dienes to afford the endoperoxide can be performed efficiently in microstructured reactors. Advantages arise from
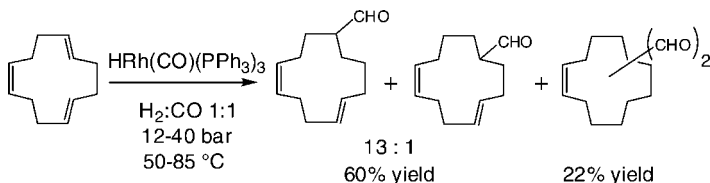
Scheme 9.5 Gas–liquid hydroformylation of cyclododecatriene in a milli-structured reactor [51].
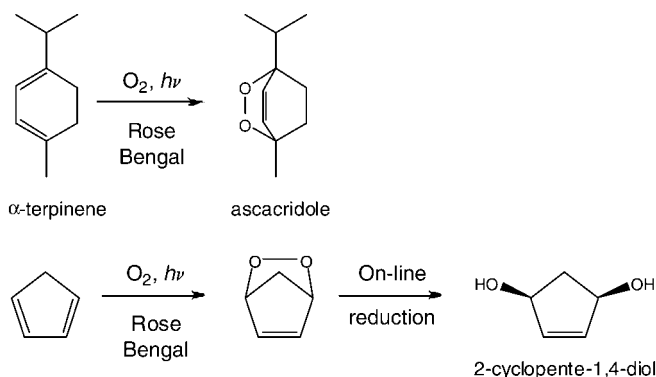
Scheme 9.6 [4 + 2] singlet oxygen addition to α-terpinene [11] and to cyclopentadiene [26].

both the short optical path due to the thin liquid layer and safety issues associated with large quantities of oxygenated organics in traditional processes. Singlet oxygen is generated by irradiation of dissolved oxygen in the presence of the photosensitizer Rose Bengal (Scheme 9.6). A single-channel etched glass microreactor, probably operating in Taylor flow, was used to perform the [4 + 2] addition to α-terpinene (ca. 0.5 g), affording ascaridole in 85% non-isolated yield using a low-intensity light source and pure oxygen at room conditions [11]. The process time to convert all of the $20\,cm^3$ of feed solution of α-terpinene in methanol is not given, but simple calculation using the liquid flow rate of $1\,\mu L\,min^{-1}$ indicate that more than 300 h are required.

A similar addition of singlet oxygen was reported for cyclopentadiene at 10–15 °C [26]. The 32-channel falling film microreactor equipped with a quartz window from the Institut für Mikrotechnik Mainz (IMM) was used for efficient gas–liquid contacting. The very reactive endoperoxide intermediate is reduced on-line with thiourea to avoid accumulation. A 20% isolated yield (0.95 g) of the 1,4-diol was obtained. Again, the process time is not given and cannot be estimated from the published data.

Ozone is a god target reagent for microreactor applications since it is toxic, difficult to handle and very reactive. A silicon-etched 16-channel ($600\,\mu m \times 300\,\mu m \times 22.7$ mm) microreactor covered with Plexiglas was used for oxidation of 1-decene into nonanal with quantitative conversion and selectivity [20]. This reaction proceeds in fact through the formation of the very reactive intermediate ozonide, which formally results from [3 + 2] addition of O_3 to the C=C bond. A consecutive reduction step with $P(OEt)_3$–EtOAc is required to yield the aldehyde. The reaction time is as short as 0.32 s. From the published data, a daily production of ca. 1600 g of nonanal per day may be obtained, which is well suited for preparation in fine chemistry.

9.3
Other H$_2$ Additions Across C=O, C≡N, C≡C, Aromatic, Nitro and O=O Bonds

Other hydrogen additions have been reported in microstructured reactors (Table 9.3). Reduction/hydrogenations of many functional groups such as carbonyls, nitriles,

Table 9.3 Other additions.

Reaction	Type	Conditions	Motivation/requirements	Substrate/product	Reactor	Reference
H$_2$ addition C=O	GLS	20 °C 21–40 bar Washcoat 1–5 min	Screening of chiral catalysts	Ethyl pyruvate	R2	[31]
	GLL	60–90 °C 20 bar Molecular 2–3 min	Selectivity Mass transfer	α,β-Unsaturated aldehydes	R3	[13]
H$_2$ addition C=O C≡N	GLS	25–90 °C 25 bar Powder 2 min	Selectivity Comparison with batch	4-Cyanobenzaldehyde	R6	[44]
H$_2$ addition quinone	GLS	20–80 °C 2–15 bar Washcoat or powder	Comparison with literature data Pilot production	Ethylanthraquinone Anthraquinone/ dihydroanthraquinone	R6 R4	[48] [40]
H$_2$ addition C≡C	GLS	25–50 °C 1 bar Washcoat 2 min	Demonstration Kinetics Selectivity	3-Methyl-1-pentyn-3-ol Diphenylacetylene 3-phenyl-2-propyn-1-ol 2-Butyne-1,4-diol	R4 R3 R6	[35] [12] [56]
H$_2$ addition aromatics	GLS	100 °C 7–8 bar Powder	Demonstration Intensification	Resorcinol to 1,3-cyclohexanedione	R8	[45, 52]

(Continued)

Table 9.3 (*Continued*)

Reaction	Type	Conditions	Motivation/requirements	Substrate/product	Reactor	Reference
Hydro-treatment	GLS	60 °C 7–25 bar Wall-coated	Demonstration Kinetics	Toluene/1-octene/styrene model feed for refining	R4	[34, 37]
H_2 addition NO_2	GLS	25–130 °C 1–32 bar Washcoat or powder 0.4–280 s	Kinetics Deactivation	Nitrobenzene	R1	[8, 38]
			Kinetics Comparison	o-Nitroanisole	R6	[46, 47]
			Demonstration	o-Nitroanisole	See text	[57]
			Demonstration	Nitrobenzene	See text	[58]
			Patent			
			Comparison	p-Nitrotoluene	R4	[59]
			Kinetics Demonstration	2,4-Dinitrotoluene	R4	[39]
H_2 addition O=O	GLS		Safety issues	Direct synthesis $H_2 + O_2 \rightarrow H_2O_2$	R3 R6 R3 –	[10] [49] [33] [60]
F_2 addition	GL	Room temperature and pressure Ni or Cu material	Exothermic Safety issues	$ArSF_3 + F_2 \rightarrow ArSF_5$	–	[61]

ethyl pyruvate

ethyl lactate
63% ee(R)

cinchonidine
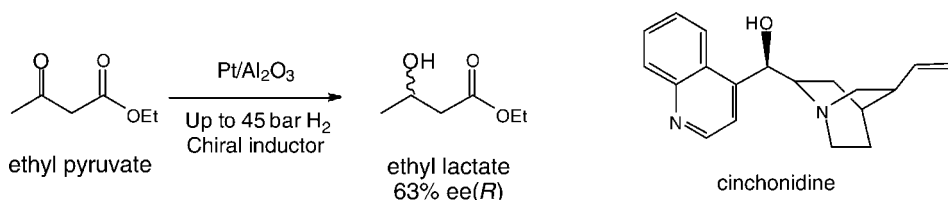
Scheme 9.7 Asymmetric heterogeneous hydrogenation of α,γ-keto esters in a microreactor [31].

quinines, alkynes and aromatics were described, in general with 3-phase (i.e. gas–liquid-solid) catalysis.

A continuous microstructured reactor equipped with a perforated (5 µm) membrane was used for the investigation of the gas–liquid-solid asymmetric hydrogenation of ethyl pyruvate to a mixture of (R)- and (S)-ethyl lactate on a Pt/γ-Al$_2$O$_3$ catalyst modified with chiral inductors under a wide range of hydrogen pressure (up to 45 bar) [31]. Eight chiral inductors were evaluated, the best enantioselectivity (63%) being obtained with cinchonidine (Scheme 9.7). The very low reaction volume (100 µL) offers short operating times. Solvent effect, deactivation studies and the effect of modifier leaching are also reported. The main drawback to a more friendly use of the mesh reactor is the difficulty in maintaining a stable gas–liquid interface, which precludes unattended operation and thus automation of the screening system.

The only example of gas–liquid–liquid reaction in a single-capillary microtube reactor has been reported by Claus's group [13]. The hydrogenation reaction is catalyzed by Ru complexed with the water-soluble version of triphenylphosphine, i.e. triphenylphosphine trisulfonate (TPPTS), under 1–2 MPa pressure at 60–90 °C. A gas–liquid–liquid segmented flow is obtained but the aqueous phase where the reaction takes place and the hydrogen bubbles are dispersed, which is likely detrimental for hydrogen mass transfer. The absence of cross-talk between the dispersed phases was used by Ismagilov and coworkers for crystallization using gas–liquid–liquid segmented flow [23]. Both the low activation energy and the dependence of the rate on the capillary diameter (500, 750 and 1000 µm) support the presence of mass transfer limitations, which translates into low conversions (< 5%).

4-Cyanobenzaldehyde was reduced with hydrogen in a packed-bed microtube reactor of 1 mm filled with small Pd/C particles under 2.5 MPa pressure and temperatures in the range 25–90 °C [44]. Both hydrogenation at the nitrile and the aldehyde occurs, leading to mixtures. Interestingly, a comparison with a batch reactor shows that a better selectivity for the amino-alcohol product (95%) is achieved in the traditional equipment. For the highest temperature, hydrogenolysis of the C−N bond occurs as expected to lead 4-methylbenzyl alcohol.

Hydrogen peroxide is mostly produced on a large scale using the anthraquinone (AQ) autoxidation process. The key step is the selective liquid-phase hydrogenation of the AQs to their corresponding hydroquinones (Scheme 9.8). An industrial process has been designed at Chalmers University and developed and used by Akzo-Nobel on the pilot scale. It involves a three-phase monolith reactor but very few details

anthraquinone (AQ)   hydroquinone (HQ)
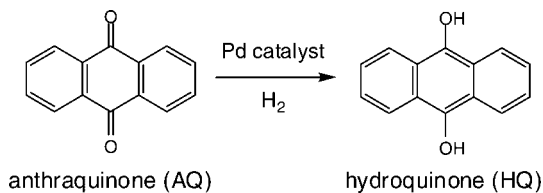
Scheme 9.8 Anthraquinone hydrogenation scheme.

regarding the channel size and geometry, the catalyst layer and the operating conditions are provided [40]. The heat of reaction is in the region of $104 \, \text{kJ mol}^{-1}$. The very similar hydrogenation of 2-ethylanthraquinone has also been evaluated in a single small-diameter ($800 \, \mu\text{m}$) packed-bed tube reactor [48].

Under ca. 7 bar pressure at $50 \, ^\circ\text{C}$, the productivity, calculated as the equivalent H_2O_2 space–time yield (STY), is 30–50 times higher in the small-diameter packed bed than in a commercial slurry reactor or in a traditional packed-bed reactor under similar operating conditions. Although the catalysts were different, the increased productivity was attributed to the higher mass transfer coefficients in the microreactor. However, the many underlying issues in scaling-up such a small laboratory reactor containing as little as 13 mg of catalyst are not mentioned.

The hydrogenation of 2-butyne-1,4-diol was carried out using a single-tube reactor of 1.65 mm i.d. operating in the Taylor segmented flow regime [56]. Selectivity in the desired 2-butene-1,4-diol of up to 95% was measured at 90% conversion. It was shown that the reactor was operating under mass transfer limitations, as demonstrated by the effect of the liquid-phase superficial velocity on the selectivity. However, hydrogen addition to carbon–carbon triple bonds is not such a challenging selectivity issue since the consecutive side-reaction leading to the non-desired saturated alkane product is blocked as long as some alkyne is present. The lower selectivities of ca. 90% obtained in this work are indeed a good demonstration of the mass transfer effect on selectivity. The situation is even worse for the hydrogenation of diphenylacetylene and 3-phenyl-2-propyn-1-ol performed in a single-channel silicon chip reactor with a wall-anchored palladium catalyst [12]. Under very smooth conditions (room temperature, 1 bar), over-reduction occurred, because the residence time was not controlled, to produce selectively the saturated derivatives 1,2-diphenylethane and 3-phenyl-1-propanol in quantitative (>97%) yields. In the latter example, not only is the benefice of using microstructured devices not demonstrated but also a negative feeling is given, because of a misunderstanding of the use of continuous flow reactors. It should be mentioned, however, that the main idea was to bring a "proof-of-principle" rather than to solve selectivity issues.

Hydrogenation of 3-methyl-1-pentyn-3-ol was performed in a monolithic stirrer reactor in which pieces of monolith were used instead of blades (Scheme 9.9). The excellent performance of ca. 90% yield in the desired 3-methyl-1-penten-3-ol is, however, comparable to that of a conventional slurry reactor [35].

A heat-exchange single-channel reactor was used for the hydrogenation of resorcinol (as the phenate sodium salt, see Scheme 9.10) [52]. The advantage of such a HEx reactor is the facility to scale up to production units while keeping the advantages of

3-methyl-1-pentyn-3-ol 3-methyl-1-penten-3-ol 3-methyl-1-pentanol
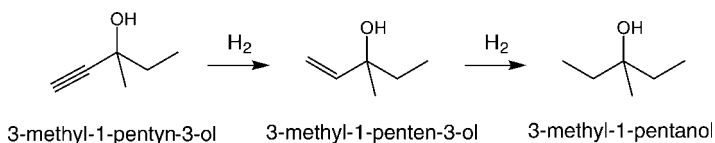
**Scheme 9.9** Reaction scheme for the hydrogenation of 3-methyl-1-pentyn-3-ol.

heat-exchange capabilities and the use of powder catalysts. In this report, catalyst screening was performed and productivity of more than $0.7 \, mol \, h^{-1} \, g^{-1}$ catalyst were measured in a laboratory single-channel reactor of 1 mm i.d. and $3 \, cm^3$ process volume. A seven-fold improvement in the rate compared with a batch reactor was reported [45]. This type of structured reactor likely represents a step towards intensified multiphase additions at the production scale. A similar study was also published on the hydrogenation addition to the carbon–carbon double bond of isophorone to trimethylcyclohexanone (Scheme 9.10) [24].

Recently, the hydrogenation a mixture of toluene, styrene and 1-octene, representing a model feed for hydrotreating in the refining industry, was performed in monolith reactors [37]. One is a γ-alumina monolith of diameter 1 cm and 15 or 30 cm long and the other is a more conventional cordierite monolith with a wall-coated layer of γ-alumina. In both monoliths, the channels size is 1–2 mm and the catalyst is based on Ni. Substantial alkene conversions of more than 50% were observed in the small-channel reactors, which was attributed to the intensified mass-transfer rate generally measured in monolith reactors [16].

The first example of nitroaromatic hydrogenation in a microstructured reactor was reported by Hönicke's group [59]. The hydrogenation of *p*-nitrotoluene at 20 bar and 97 °C was used to compare different structures such as a channeled (14 channels, $300 \, \mu m \times 700 \, \mu m \times 4 \, cm$) aluminum wafer, aluminum wires and a traditional fixed-bed reactor (FB). Much higher conversions, up to 85% in the FB compared with 58% in the channels, were obtained because of the higher exposed surface area (BET) of the 1% Pd/alumina catalyst in the FB compared with that of the wall-coated microstructured wafer. Gavriilidis's group performed the hydrogenation of nitrobenzene to aniline in ethanol at medium temperature (60 °C) and pressure (1–4 bar) [8, 28]. Conversions of up to 100% were measured with residence times as short as 9–17 s. Deactivation of the palladium catalyst was investigated as a function of the method used for deposition: sputtering, UV decomposition of palladium acetate, incipient wetness or impregnation. One main cause of deactivation was attributed to deposition

resorcinol 1,3-cyclohexanedione isophorone trimethylcyclohexanone
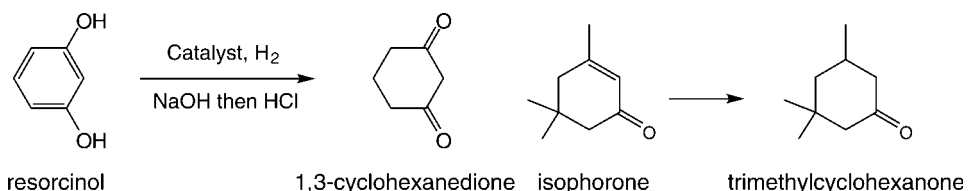
Scheme 9.10 Reagents and products for the reactions performed with the HEx reactor.
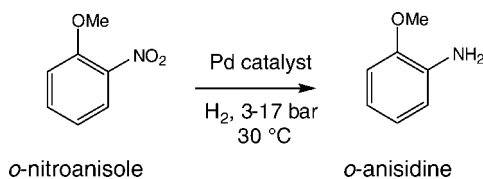
Scheme 9.11 Hydrogenation of *o*-nitroanisole.

of organic compounds. In such a case, activity could be recovered by oxidation at 130 °C. Palladium loss was also observed. Total conversions and selectivities of more than 85% were obtained with the impregnated palladium catalyst for times on-stream of up to 10 h. In their conclusion, the authors proposed a comparison between the productivity of the micro-falling film unit and a batch reactor working at higher pressure (20 bar) and temperature (125 °C). Although the microreactor displays a two-fold increase in productivity (ca. 400 kmol$_{aniline}$ m$_{reactor}^{-3}$ per day) compared with the batch (ca. 200 kmol$_{aniline}$ m$_{reactor}^{-3}$ per day), issues concerning the management of catalyst deactivation and that dealing with scale-up of the microreactor volume from ca. 100 µL to 1 m^3 were not raised [28].

Comparison of a single-tube packed-bed reactor with a traditional batch reactor was also published in the case of *o*-nitroanisole hydrogenation, not for productivity purposes but rather as laboratory tools for kinetic studies (Scheme 9.11) [46]. It was shown that the better efficiency of mass transfer enables the microreactor to obtain intrinsic kinetic data for fast reactions with characteristic times in the range 1–100 s, under isothermal conditions, which is difficult to achieve with a stirred tank reactor. However, the batch reactor used in this study was not very well designed since a maximum mass transfer coefficient (k_la) of only 0.06 s^{-1} was measured at 800 rpm, whereas k_la values of up to 2 s^{-1} are easily achieved in small stirred tank reactors equipped with baffles and mechanically driven impellers [25]. This questions the reference used when comparing microstructured components with traditional equipment, with the conclusion that comparison holds only when the best traditional technology is used.

A catalyst-trap microreactor etched in silicon was used also for the hydrogenation of *o*-nitroanisole at 30 °C, ca. 2 bar and 0.06–0.5 cm^3 min^{-1} [57]. No side-reactions occur, as shown by the total (ca. 100%) selectivity towards *o*-anisidine. The catalyst particles (Pd/C 5% w/w, 35–50 µm) are held in a trapezoidal arrangement of four posts. Although the total catalyst loading was not provided, it is less than 13% since a void fraction of 87% is reported. This is much less than the 50% catalyst hold-up generally observed in fixed-bed reactors. The scale-up and heat transfer issues for this "high tech" microstructured reactor with a channel volume of ca. 100 mm^3 are, however, not tackled. The idea of using posts to trap and/or control the formation of a well-defined catalytic bed was also developed for the hydrogenation of nitrobenzene on a Pd/C catalyst [58]. With a 20 × 20 × 1 mm cavity (400 µL), the liquid throughput in this reactor is likely higher and a heat exchange plate has been incorporated. Further, ceramic monolith reactors may also be used for nitroaromatic hydrogenation [39]. A simulation performed with a 400 cpsi monolith (channels of 1.1 mm i.d.)

for single-pass reaction reveals a lower pressure drop, higher mass transfer and plug flow behavior, thus leading to higher productivity. However, the temperature profile in the monolith is rather high (50 °C), indicating some external heat transfer limitations. due to the exothermic reaction (ca. 550 kJ mol^{-1}) but performed at a rather low reagent concentration (0.14 kmol m^{-3}). Simulated 2,4-dinitrotoluene conversions (>99%) and 4-toluenediamine yields (>96%) are high. Note, however, that the formation of azoxy or other side-products was not included in the simulation, which is therefore not able to predict the effect of the temperature gradient on the selectivity.

The anthraquinone (AQ) autoxidation process discussed above to produce hydrogen peroxide presents serious drawbacks and many studies have been devoted to the direct process, i.e. the direct synthesis of hydrogen peroxide from addition of H_2 to O_2. Typical conditions involve the use of a supported palladium catalyst in a liquid mixture of sulfuric acid, phosphoric acid and bromide, the composition being important to stabilize the hydrogen peroxide formed. A patent reported the fabrication of H_2O_2 in a solvent containing water, NaBr and H_2SO_4, catalyzed by Pd/C, with an oxygen flow rate of 0.25–5 dm^3 h^{-1} at 83 °C [60]. In order both to achieve rapid mixing and to operate under safe conditions without explosion, a microstructured cyclone-type gas–liquid mixer of typical dimensions 200 μm was used, but no details were provided concerning the contact between the catalyst and the gas–liquid mixture. Although the H_2O_2 yields are not indicated, it is demonstrated that an $H_2 : O_2$ ratio close to unity is preferable. The direct synthesis was also investigated in the explosive regime (2–3 MPa, 20 °C) by Jensen's group at MIT in a micro packed-bed reactor featuring 10 parallel channels with a Pd/C powder catalyst [33]. At a total gas flow rate in the range 2–15 cm^3 min^{-1} and a liquid flow rate of 0.1 cm^3 min^{-1}, corresponding to a residence time in the region of 20 s, the conversion of H_2 was about 5% with quantitative selectivity in H_2O_2, i.e. avoiding the problem of water formation [33]. A microstructured reactor featuring gas–liquid Taylor flow in wash-coated single- and multi-channel designs, using hydrochloric acid and KBr in the liquid layer and a palladium catalyst, was also reported. Again, the conversion was kept low (5%) with a productivity of ca. 3 mol$_{H_2O_2}$ mol$_{Pd}^{-1}$ h^{-1} [10]. The year 2007 was very rich for direct syntheses, with a further publication dealing with a micro packed-bed Pd/C single-tube reactor (765 μm i.d.) containing 2% Pd/SiO$_2$ catalyst particles (75 and 150 μm) up to ca. 2 MPa total pressure and 50 °C [49]. The set-up was used to determine a Langmuir–Hinshelwood kinetic model with an activation energy of 22 kJ mol^{-1}.

9.4
Miscellaneous Additions

A single-channel (500 μm × 500 μm × 70 mm) microreactor has been designed for use with elemental fluorine, both for selective fluorination and for perfluorination of organic compounds [61]. The addition of fluorine to the trifluorosulfur group leads to the pentafluoro derivative in 44% yield (Scheme 9.12). From the data indicating that
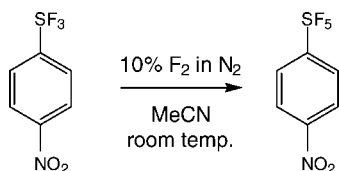
Scheme 9.12 Fluorine addition to the trifluorosulfur group yielding the pentafluoro derivative [61].

annular flow prevails with a low liquid hold-up in the channel, a reaction time of <10 s can be estimated.

9.5
Conclusion

Only very few addition reactions have been performed using microstructured devices, with a large predominance of hydrogenations. This is surprising since microreaction technology offers the possibility to fulfill the many requirements of most multiphase addition reactions such as large exotherms up to 500 kJ mol^{-1}, high external mass transfer coefficients, short residence time, high pressure and temperature, and safety issues. Several considerations may explain this fact. First, it is believed that well-defined, mastered and flexible multiphase contacting in microstructured devices is not commercially available, with the exception of the micro-falling film reactor (**R1**). Second, the throughputs offered are not high enough, even for small-scale production, and scale-up issues are often not foreseen. Third, comparison with traditional equipment is seldom performed, and/or when performed are not fair in the sense that poorly performing standard equipment is chosen as references and/or the comparison criteria are not adapted (e.g. production per cubic meter of reactor). However, many multiphase additions have a potential to benefit microreaction technologies. Reductions in mass and heat transfer should result in a reduction in the reaction inventory and should benefit additions involving dangerous and toxic reagents (HCN for hydrocyanation, CO for carbonylation and hydroformylation) which present exothermicity in the range 100–200 kJ mol^{-1}.

References

1 V. Hessel, P. Angeli, A. Gavriilidis, H. Löwe, Gas-liquid and gas–liquid-solid microstructured reactors: contacting principles and applications, *Ind. Eng. Chem. Res.* **2005**, *44*, 9750–9769.

2 A. Gavriilidis, P. Angeli, E. Cao, K. K. Yeong, Y. S. S. Wan, Technology and applications of microengineered reactors, *Chem. Eng. Res. Des.* **2002**, *80* (A1), 3–30.

3 G. N. Doku, W. Verboom, D. N. Reinhoudt, A. van den Berg, On-microchip multiphase chemistry – a review of microreactor design principles and reagent contacting modes, *Tetrahedron* **2005**, *61*, 2733–2742.

4 C. de Bellefon, N. Pestre, Chemical engineering aspects of homogeneous hydrogenations, in *Handbook of*

Homogeneous Hydrogenations (ed. J. G. de Vries and C. J. Elsevier), Wiley-VCH Verlag GmbH, **2006**, Vol. 3, Chapter 45, pp. 1517–1546.

5 V. Meille, Review on methods to deposit catalysts on structured surfaces, *Appl. Catal. A* **2006**, *23*, 1–17.

6 IMM, http://www.imm-mainz.de/upload/dateien/Catalogue5_06_FFMR.pdf.

7 P. Löb, H. Löwe, V. Hessel, Fluorination, chlorinations and brominations of organic compounds in micro reactors, *J. Fluorine Chem.* **2004**, *125*, 1677–1694.

8 K. K. Yeong, A. Gavriilidis, R. Zapf, V. Hessel, Experimental studies of nitrobenzene hydrogenation in a microstructured falling film reactor, *Chem. Eng. Sci.* **2004**, *59*, 3491–3494.

9 J. Shaw, C. Turner, B. Miller, M. Harper, Reaction and transport coupling for liquid and liquid/gas microreactor systems, in *IMRET 2, Process Miniaturization, 2nd International Conference on Microreactor Technology, AIChE Meeting*, New Orleans, Topical Conference Preprint (AIChE) **1998**, pp. 176–180.

10 X. Wang, Y. Nie, J. L. C. Lee, S. Jaenicke, Evaluation of multiphase microreactors for the direct formation of hydrogen peroxide, *Appl. Catal. A* **2007**, *317*, 258–265.

11 R. C. R. Wootton, R. Fortt, A. J. de Mello, A microfabricated nanoreactor for safe, continuous generation and use of singlet oxygen, *Org. Process Res. Dev.* **2002**, *6*, 187–189.

12 J. Kobayashi, Y. Mori, K. Okamoto, R. Akiyama, M. Ueno, T. Kitamori, S. Kobayashi, A microfluidic device for conducting gas–liquid–solid hydrogenation reactions, *Science* **2004**, *304*, 1305–1308.

13 Y. Önal, M. Lucas, P. Claus, Application of a capillary microreactor for selective hydrogenation of α,β-unsaturated aldehydes in aqueous multiphase catalysis, *Chem. Eng. Tech.* **2005**, *28*, 972–978.

14 S. Roy, T. Bauer, M. Al-Dahhan, P. Lehner, T. Turek, Monoliths as multiphase reactors, *AIChE J.* **2004**, *50*, 2918–2938.

15 A. Cybulski, J. A. Moulijn, *Structured Catalysts and Reactors*, 2nd edn, Taylor and Francis, London, **2006**.

16 M. T. Kreutzer, F. Kapteijn, J. A. Moulijn, J. J. Heiszwolf, Multiphase monolith reactors: chemical reaction engineering of segmented flow in microchannels, *Chem. Eng. Sci.* **2005**, *60*, 5895–5916.

17 M. W. Losey, M. A. Schmidt, K. F. Jensen, Microfabricated multiphase packed bed reactors: characterization of mass transfer and reaction, *Ind. Eng. Chem. Res.* **2001**, *40*, 2555–2562.

18 S. Tadepalli, D. Qian, A. Lawal, Comparison of performance of microreactor and semi-batch reactor for catalytic hydrogenation of *o*-nitroanisole, *Catal. Today* **2007**, *125*, 64–73.

19 R. D. Oleschuk, L. L. Shultz-Lockyear, Y. Ning, D. J. Harrison, Trapping of bead-based reagents within microfluidic systems. On-chip solid-phase extraction and electrochromatography, *Anal. Chem.* **2000**, *72*, 585–590.

20 Y. Wada, M. A. Schmidt, K. F. Jensen, Flow distribution and ozonolysis in gas–liquid multichannel microreactors, *Ind. Eng. Chem. Res.* **2006**, *45*, 8036–8042.

21 L. Kiwi-Minsker, A. Renken, Microstructured reactors for catalytic reactions, *Catal. Today* **2005**, *110*, 2–14.

22 M. Alame, N. Pestre, C. de Bellefon, Extensive re-investigations of pressure effects in Rh catalyzed asymmetric hydrogenations, *Adv. Synth. Catal.* **2008**, *350*, 898–908.

23 D. L. Chen, L. Li, S. Reyes, D. N. Adamson, R. F. Ismagilov, Using three-phase flow of immiscible liquids to prevent coalescence of droplets in microfluidic channels: criteria to identify the third liquid and validation with protein crystallization, *Langmuir* **2007**, *23*, 2255–2260.

24 D. I. Enache, G. J. Hutchings, S. H. Taylor, E. H. Stitt, The hydrogenation of isophorone to trimethyl cyclohexanone using the downflow single capillary reactor, *Catal. Today* **2005**, *105*, 569–573.

25 V. Meille, N. Pestre, P. Fongarland, C. de Bellefon, Gas–liquid mass transfer in small laboratory batch reactors: comparison of methods, *Ind. Chem. Eng. Res.* **2004**, *43*, 924–927.

26 K. Jähnisch, U. Dingerdissen, Photochemical generation and [4 + 2]-cycloaddition of singlet oxygen in a falling-film micro reactor, *Chem. Eng. Tech.* **2005**, *28*, 426–427.

27 J. W. Lee, K. K. Yeong, A. Gavriilidis, R. Zapf, V. Hessel, Catalyst stabilization for cyclohexane hydrogenation in a microstructured falling film reactor, in *Proceedings of AIChE Spring Nationnal Meeting, IMRET 8,* Atlanta, GA, **2005.**

28 K. K. Yeong, A. Gavriilidis, R. Zapf, V. Hessel, Catalyst preparation and deactivation issues for nitrobenzene hydrogenation in a microstructured falling film reactor, *Catal. Today* **2003**, *81*, 641–651.

29 D. A. Wenn, J. E. A. Shaw, B. Mackenzie, A mesh microcontactor for 2-phase reactions, *Lab Chip* **2003**, *3*, 180–186.

30 R. Abdallah, V. Meille, J. Shaw, D. Wenn, C. de Bellefon, Gas–liquid and gas–liquid–solid catalysis in a mesh microreactor, *Chem. Commun.* **2004**, 372–373.

31 R. Abdallah, B. Fumey, V. Meille, C. de Bellefon, Micro-structured reactors as a tool for chiral modifier screening in gas–liquid–solid asymmetric hydrogenations, *Catal. Today* **2007**, *125*, 34–39.

32 R. Abdallah, P. Magnico, B. Fumey, C. de Bellefon, CFD and kinetic methods for mass transfer determination in a mesh microreactor, *AIChE J.* **2006**, *52*, 2230–2237.

33 T. Inoue, M. A. Schmidt, K. F. Jensen, Microfabricated multiphase reactors for the direct synthesis of hydrogen peroxide from hydrogen and oxygen, *Ind. Eng. Chem. Res.* **2007**, *46*, 1153–1160.

34 W. Liu, S. Roy, Effect of channel shape on gas/liquid catalytic reaction performance in structured catalyst/reactor, *Chem. Eng. Sci.* **2004**, *59*, 4927–4939.

35 I. Hoek, T. A. Nijhuis, A. I. Stankiewicz, J. A. Moulijn, Performance of the monolithic stirrer reactor: applicability in multi-phase processes, *Chem. Eng. Sci.* **2004**, *59*, 4975–4981.

36 W. Liu, W. P. Addiego, C. M. Sorensen, T. Boger, Monolith reactor for the dehydrogenation of ethylbenzene to styrene, *Ind. Eng. Chem. Res.* **2002**, *41*, 3131–3138.

37 W. Liu, S. Roy, X. Fu, Gas–liquid catalytic hydrogenation reaction in small catalyst channel, *AIChE J.* **2005**, *51*, 2285–2297.

38 R. P. Fishwick, R. Natividad, R. Kulkarni, P. A. McGuire, J. Wood, J. M. Winterbottom, E. H. Stitt, Selective hydrogenation reactions: a comparative study of monolith CDC, stirred tank and trickle bed reactors, *Catal. Today* **2007**, *128*, 108–114.

39 M. T. Kreutzer, F. Kapteijn, J. A. Moulijn, Fast gas–liquid–solid reactions in monoliths: a case study of nitro-aromatic hydrogenation, *Catal. Today* **2005**, *105*, 421–428.

40 R. Edvinsson Albers, M. Nyström, M. Siverström, A. Sellin, A. -C. Dellve, U. Andersson, W. Herrmann, Th. Berglin, Development of a monolith-based process for H$_2$O$_2$ production: from idea to large-scale implementation, *Catal. Today* **2001**, *69*, 247–252.

41 C. de Bellefon, R. Abdallah, T. Lamouille, N. Pestre, S. Caravieilhes, P. Grenouillet, High Throughput Screening of molecular catalysts using automated liquid handling, injection and microdevices, *Chimia* **2002**, *56*, 621–626.

42 C. de Bellefon, N. Pestre, T. Lamouille, P. Grenouillet, V. Hessel, High Throughput Kinetic Investigations of Asymmetric Hydrogenations with Microdevices, *Adv. Synth. Catal.* **2003**, *345*, 190–193.

43 C. de Bellefon, N. Tanchoux, S. Caravieilhes, P. Grenouillet, V. Hessel, Microreactors for dynamic high throughput screening of fluid–liquid catalysis, *Angew. Chem. Int. Ed.* **2000**, *39*, 3442–3445.

44 N. Yoswathananont, K. Nitta, Y. Nishiuchi, M. Sato, Continuous hydrogenation reactions in a tube reactor packed with Pd/C, *Chem. Commun.* **2005** 40–42.

45 D. I. Enache, G. J. Hutchings, S. H. Taylor, R. Natividad, S. Raymahasay, J. M. Winterbottom, E. H. Stitt, Experimental evaluation of a three-phase downflow capillary reactor, *Ind. Eng. Chem. Res.* **2005**, *44*, 6295–6303.

46 S. Tadepalli, R. Halder, A. Lawal, Catalytic hydrogenation of *o*-nitroanisole in a microreactor: reactor performance and kinetic studies, *Chem. Eng. Sci.* **2007**, *62*, 2663–2678.

47 S. Tadepalli, D. Qian, A. Lawal, Comparison of performance of microreactor and semi-batch reactor for catalytic hydrogenation of *o*-nitroanisole, *Catal. Today* **2007**, *125*, 64–73.

48 R. Halder, A. Lawal, Experimental studies on hydrogenation of anthraquinone derivative in a microreactor, *Catal. Today* **2007**, *125*, 48–55.

49 Y. Voloshin, R. Halder, A. Lawal, Kinetics of hydrogen peroxide synthesis by direct combination of H_2 and O_2 in a microreactor, *Catal. Today* **2007**, *125*, 40–47.

50 F. Trachsel, C. Hutter, Ph. Rudolf von Rohr, Transparent silicon/glass microreactor for high-pressure and high-temperature reactions, *Chem. Eng. J.* **2008**, *135*, S309–S316.

51 D. I. Enache, W. Thiam, D. Dumas, S. Ellwood, G. J. Hutchings, S. H. Taylor, S. Hawker, E. H. Stitt, Intensification of the solvent-free catalytic hydroformylation of cyclododecatriene: comparison of a stirred batch reactor and a heat-exchange reactor, *Catal. Today* **2007**, *128*, 18–25.

52 D. I. Enache, G. J. Hutchings, S. H. Taylor, S. Raymahasay, J. M. Winterbottom, M. D. Mantle, A. J. Sederman, L. F. Gladden, C. Chatwin, K. T. Symonds, E. H. Stitt, Multiphase hydrogenation of resorcinol in structured and heat exchange reactor systems: influence of the catalyst and the reactor configuration, *Catal. Today* **2007**, *128*, 26–35.

53 C. de Bellefon, T. Lamouille, N. Pestre, F. Bornette, H. Pennemann, F. Neumann, V. Hessel, Asymmetric catalytic hydrogenations at micro-litre scale in a helicoidal single channel falling film microreactor, *Catal. Today* **2005**, *110*, 179–187.

54 S. Caravieilhes, C. de Bellefon, N. Tanchoux, Dynamic methods and new reactors for liquid phase molecular catalysis, *Catal. Today* **2001**, *66*, 145–155.

55 E. Dietzsch, J. Mueller, N. Voelkel, E. Klemm, Microreactor concepts for enhanced mass transfer in the two-phase hydroformylation of 1-octene, in *DGMK Tagungsbericht (2006), 2006–4, Proceedings of the DGMK/SCI-Conference "Synthesis Gas Chemistry"*, **2006**, pp. 163–169.

56 A. N. Tsoligkas, M. J. H. Simmons, J. Wood, C. G. Frost, Kinetic and selectivity studies of gas–liquid reaction under Taylor flow in a circular capillary, *Catal. Today* **2007**, *128*, 36–46.

57 S. McGovern, G. Harish, C. S. Pai, W. Mansfield, J. A. Taylor, S. Pau, R. S. Besser, Multiphase flow regimes for hydrogenation in a catalyst-trap microreactor, *Chem. Eng. J.* **2008**, *135*, S229–S236.

58 P. Pfeifer, K. Haas-Santo, K. Schubert, Micro-structured reactor with catalyst bed used for the 2-phase hydrogenation of nitrobenzene, German Patent DE102005022958, **2006**.

59 R. Födisch, D. Hönicke, Y. Xu, B. Platzer, Heterogeneously catalyzed liquid-phase hydrogenation of nitro-aromatics using microchannel reactors, in *Proceedings of IMRET5*, **2001**, pp. 470–478.

60 K. M. Vanden Bussche, S. F. Abdo, A. R. Oroskar, to UOP LLC, US Patent 6 713 036, filed 2001, published **2004**.

61 R. D. Chambers, R. C. H. Spink, Microreactors for elemental fluorine, *Chem. Commun.* **1999**, 883–884.